

NASA Contractor Report 189058
IEPC-91-038

1N-20
61955
P-16

Mission and System Optimization of Nuclear Electric Propulsion Vehicles for Lunar and Mars Missions

James H. Gilland
Sverdrup Technology, Inc.
Lewis Research Center Group
Brook Park, Ohio

December 1991

Prepared for
Lewis Research Center
Under Contract NAS3-25266



(NASA-CR-189058) MISSION AND SYSTEM
OPTIMIZATION OF NUCLEAR ELECTRIC PROPULSION
VEHICLES FOR LUNAR AND MARS MISSIONS Final
Report (Sverdrup Technology) 16 p CSCL 21H

N92-15124

Unclass
0061955

63/20

Mission and System Optimization of Nuclear Electric Propulsion Vehicles for Lunar and Mars Missions

James H. Gilland*
Sverdrup Technology, Inc.
Lewis Research Center Group
Brook Park, Ohio 44142

Abstract

The detailed mission and system optimization of low thrust electric propulsion missions is a complex, iterative process involving interaction between orbital mechanics and system performance. Through the use of appropriate approximations, initial system optimization and analysis can be performed for a range of missions. The intent of these calculations is to provide system and mission designers with simple methods to assess system design without requiring access or detailed knowledge of numerical, calculus of variations optimization codes and methods. Approximations for the mission/system optimization of Earth orbital transfer and Mars missions have been derived. Analyses include the variation of thruster efficiency with specific impulse. Optimum specific impulse, payload fraction, and power/payload ratios are calculated. The accuracy of these methods is tested and found to be reasonable for initial scoping studies. Results of optimization for Space Exploration Initiative lunar cargo and Mars missions are presented for a range of power system and thruster options.

Symbols

a	Acceleration
c	Exhaust Velocity
g_0	Gravitational Acceleration, 9.81 m/s ²
I_{sp}	Specific Impulse, c/ g_0
J	Low Thrust Mission Parameter, $\int a^2 dt$
P_e	Electric Power Input to Thrusters
P_j	Jet Power, Thrust*Exhaust velocity/2
M_l	Payload Mass
M_0	Initial Mass
M_p	Mass of Planet
M_{pp}	Propellant Mass
M_{ps}	Total Power and Propulsion System Mass
MF	Mass Fraction, Final Mass/Initial Mass: $(M_l + M_{ps})/M_0$
R	Circular Orbit Radius, m
TF	Tankage Fraction, Tank Mass/ M_{pp}
V	Circular Orbital Velocity, $\sqrt{GM_p/R}$
α	Power and Propulsion System Specific Mass, M_{ps}/P_e
μ	Payload Fraction, M_l/M_0
η	Thruster efficiency, P_j/P_e
ΔV	Velocity Increment

*Research Engineer, Aerospace Analysis Section, Member, AIAA.

This paper is declared a work of the U.S. Government and is not subject to copyright protection in the United States.

Introduction

A recent, burgeoning interest in the human exploration of the Moon and Mars has introduced demanding requirements upon future propulsion systems. Specific missions of interest to the Space Exploration Initiative (SEI) include piloted and cargo lunar and Mars missions. In order to perform such missions in a cost effective manner, high specific impulses (I_{sp}) and low mass propulsion systems are needed. Among the candidate propulsion concepts, electric propulsion, in particular Nuclear Electric Propulsion (NEP), promises to enable both mass efficient cargo vehicle and fast lightweight piloted vehicle applications^{1,2}.

Advanced SEI missions are characterized by relatively large payload mass requirements, and, in the case of the piloted missions, relatively fast travel times. These traits combine to require significant advances in the state of the art in electric propulsion. Increased space power system and thruster power levels, I_{sp} levels, and reduced propulsion system specific mass are needed to accomplish SEI mission goals effectively using electric propulsion.

Electric propulsion systems introduce additional degrees of complexity into both systems design and optimization as well as mission analysis. Unlike traditional high-thrust systems, the nature of low-acceleration propulsion systems requires a close coupling of system assumptions with trajectory

analysis. This coupling results in an iterative, two level optimization of system performance and trajectory. This problem is particularly difficult in the case of interplanetary missions, where trajectory optimization of electric propulsion systems requires numerical integration of the equations of motion, a computationally intensive procedure. In addition, the optimal trajectory solution is affected by the system performance assumptions input into the equations of motion.

Earth Orbital Transfer/Lunar Cargo Missions

Mission Analysis

Earth orbital missions using low thrust propulsion form a unique subset of the trajectory analysis problem. These missions are unique in that the Earth's gravity (1 - .1 g) is significantly greater than the acceleration generated by the electric propulsion systems ($\sim 10^{-4}$ g), allowing for simplification and linearization of the trajectory analysis. The result of such an analysis is that a low acceleration orbital transfer from one orbit to another can be based on a constant velocity increment, in much the same way that an impulsive, high thrust chemical or nuclear thermal system can. The simplified equation for orbital transfer is expressed as³

$$\Delta V^2 = V_1^2 + V_2^2 - 2V_1 V_2 \cos(\pi \Delta \Theta / 2) \quad (1)$$

Where

V_1 = Initial circular orbital velocity

V_2 = Final circular orbital velocity

$\Delta \Theta$ = Inclination change ($^\circ$)

The assumption of constant ΔV allows the rocket equation for a power limited system to be used for mission/system optimization⁴

$$e^{\Delta V/c} = (\mu + TF + \alpha c^2 / (2\eta t)) / (1 + TF + \alpha c^2 / (2\eta t)) \quad (2)$$

Equation 4 assumes that the vehicle mass consists of payload, propulsion system, propellant, and tankage. The t term represents thrusting time, which is equivalent to trip time for NEP missions. The equation can be solved for payload fraction, and differentiated with respect to exhaust velocity. The resulting equation, when equated with zero, can then be solved for the exhaust velocity that yields the maximum payload fraction:

$$d\mu/dc = \{\alpha c/\eta t - ((d\eta/dc)(\alpha c^2/2\eta t))\} \{e^{\Delta V/c} - 1\} + (\Delta V/c^2)e^{\Delta V/c}(1 + TF + \alpha c^2/(2\eta t)) = 0 \quad (3)$$

This derivation has been performed previously for orbital transfer missions⁴. In this past effort, the transcendental nature of the equation was thought to require a graphical solution for optimal I_{sp} . It has been found, however, that a suitably accurate solution, reflecting the effects of both system performance and mission ΔV , can be obtained using a second order approximation of the exponential term:

$$e^{\Delta V/c} \sim 1 + \Delta V/c + (1/2)(\Delta V/c)^2.$$

System Optimization

As noted above, another critical function that must be modelled in the optimal solution is the thruster efficiency function, η . Although a solution can be obtained for constant efficiency, the more applicable and useful solution includes the effects of efficiency variation in the analysis. Two forms of efficiency function were used in this analysis. The first function corresponds closely to ion propulsion performance and is commonly expressed as

$$\eta = bc^2/(c^2 + d^2) \quad (4)$$

with b (dimensionless) and d (m/s) obtained from theoretical models and experimental data^{5,6,7}. Three ion thruster propellants were considered: argon, krypton, and xenon. Table 1 shows the efficiency coefficients for each of these propellants. The values indicated are projections of the upper bound in ion thruster performance based on current experiments with low power thrusters.

Table 1. Ion Thruster Efficiency Parameters.

Propellant	b	d (m/s)	I_{sp} Range (s)
Xe	.86	11900	3000 - 5000
Kr	.86	15000	4000 - 7000
A	.84	22500	5000 - 10000

The second efficiency form was derived to represent MPD thruster behavior, based on a model of self-field thruster performance using an Alfvén velocity limitation model derived by Choueiri^{6,8}. The experimental parameter space of mass flow rate, current, and voltage used in the original modelling were converted to system variables such as power, specific impulse, and efficiency for use in optimization of NEP systems. The efficiency values used in this analysis represent projections of MPD thruster performance

using hydrogen propellant, assuming improved efficiency through the use of applied fields or innovative thruster geometries. The resulting efficiency equations take the form

$$\eta = bc/(c + d) \text{ (partially ionized, } I_{sp} < 7800 \text{ s)} \quad (5a)$$

$$\eta = bc^2/(c^2 + d^2) \text{ (fully ionized, } I_{sp} > 7800 \text{ s)} \quad (5b)$$

The projected values of b and d for each equation are shown in Table 2. These parameters represent projected MPD thruster performance; experimental and analytical effort will be required to determine the actual performance limits of the MPD thruster in terms of efficiency, maximum I_{sp} , and design. The forms of the optimum specific impulse equations were found to depend upon the functional form of the efficiency - I_{sp} relation. An analytical solution is possible for either form of efficiency function.

Table 2. Hydrogen MPD Thruster Efficiency Parameters.

	$\frac{b}{c}$	$\frac{d(m/s)}{c}$
$I_{sp} < 7800 \text{ s}$.86	25900
$I_{sp} > 7800 \text{ s}$.92	50300

Substituting the efficiency equations into Equation 3 yields the optimal specific impulse as a function of trip time, specific mass, and ΔV . The resulting optimum exhaust velocity ($I_{sp} * g_0$) equations are expressed in terms of ΔV , specific mass (α), trip time (t), and the b and d coefficients in the efficiency equations:

$$c_{opt} = -\Delta V/2 + \sqrt{((\Delta V/2)^2 + (1+TF)2bt/\alpha + d^2)} \quad (6a)$$

$$c_{opt} = -\Delta V/2 + \sqrt{((\Delta V/2)^2 + (1+TF)2bt/\alpha - d\Delta V/2)} \quad (6b)$$

Equation 6a is used for the quadratic efficiency functional form seen in the case of the ion and fully ionized MPD thrusters. Equation 6b is for the more linear partially ionized MPD thruster efficiency function. In addition, the optimum power requirement can also be calculated, normalized by payload mass, using the expression

$$P_e/M_1 = (1 - e^{-\Delta V/c})c^2/((2\eta\mu)) \quad (7)$$

Therefore, optimal orbital transfer vehicle performance (power, I_{sp}) can be calculated for a given payload and trip time.

Results of these equations have compared to the

actual optimums calculated using equation (2) for varying I_{sp} . The greatest error occurs at low trip times, where $\Delta V/c$ approaches values closer to 1. In the short trip regime, the error was found to be ~10%. Better agreement was obtained for the longer trip times. It should be noted slight differences in I_{sp} generally did not result in drastic changes in payload fraction or power results, due to the relatively low ΔV of the mission.

Power and Propulsion System Assumptions for Calculations

Two values of specific mass are considered, 10 and 20 kg/kWe. This specific mass is assumed to include reactor, shield, power conversion, heat rejection, power processing, and thruster subsystems. The lower value is representative of a nuclear power source using SP-100 reactor technology with a potassium Rankine dynamic power conversion system. The higher value is intended to represent a Brayton cycle option, which suffers from a greater radiator mass penalty than the Rankine systems⁹. As stated previously, a variety of thruster and propellant options can be considered for the lunar cargo vehicle. The sensitivity to specific mass and to thruster performance will be shown in the accompanying data.

Optimization Results

Some representative systems optimizations have been performed for the lunar mission. It is not the intent of these analyses to identify specific mission or technology efforts for the SEI program; rather, the results presented here are intended to illustrate the studies that are possible using the optimization methods outlined above. Technology assumptions were chosen to be representative of systems of interest. No tankage fraction was assumed in these calculations, as the proper values for the various propellants are not yet well known for SEI missions, and the issue of tank jettison arises to complicate the mission comparisons. Equations 6 show the effect of tankage fraction upon the optimization. For non-zero values of tankage fraction, higher values of specific impulse are optimum, with correspondingly higher values for power.

The optimum I_{sp} , payload fraction, and normalized power data for one-way trips using a 10 kg/kWe power/propulsion system are shown in Figures 1, 3, and 5. Figures 2, 4, and 6 show the same performance at 20 kg/kWe. Calculations for ion and MPD thrusters are shown in each figure for comparison. These calculations were performed with no more detailed

modeling of the thrusters than the I_{sp} - efficiency relations; the physical limits of the thrusters based on engineering and lifetime issues must be considered in conjunction with the optimized data to determine feasible applications of these thrusters.

Observations on Relative Propulsion System Performance

Specific Impulse The optimal I_{sp} ranges vary with trip time for a given specific mass, representing a trade off between propellant mass and power system mass in optimizing the vehicle. The optimal I_{sp} ranges for the three thrusters and both specific masses are shown in Table 3.

In order to obtain a meaningful interpretation of the optimum specific impulse values, the results of the calculations must be compared with the actual performance capabilities of each thruster and propellant combination as stated in Table 1. The optimal I_{sp} results are dependent on both trip time and specific mass, with higher I_{sp} values desirable for long trip times and low α values. Minimum trip times are determined by the I_{sp} limits for a given thruster and propellant.

Table 3. Optimal Specific Impulse Ranges for Lunar Cargo Vehicles.

<u>Thruster</u>	<u>I_{sp} (s)</u>	
	<u>10 kg/kWe</u>	<u>20 kg/kWe</u>
Ion		
Xenon	2000-7000	1800-6800
Krypton	2200-7200	2100-6900
Argon	3000-7400	2800-7000
MPD	2200-7000	1400-6600

An argon specific impulse lower limit of 5000 seconds results in optimal lunar transfer solutions for trip times of 150 days or more at 10 kg/kWe, and 300 days or more at 20 kg/kWe. Below these trip times, realistic analyses of argon ion thrusters would require fixing I_{sp} at 5000 seconds and increasing power levels, with a concomitant decrease in payload fraction over the optimal solution. Similar limits for xenon thrusters are 70 (10 kg/kWe) and 140 days (20 kg/kWe). Krypton thruster limits are 120 (10 kg/kWe) and 200 days (20 kg/kWe). The MPD thruster has the capability of operating at specific impulses as low as 2000 s, and so can be operated optimally at trip times as low as 40 to 80 days.

Based on the optimal solutions, the xenon and krypton ion and hydrogen MPD thrusters show the greatest potential for high payload fraction, moderate trip time, and low power operation of a lunar cargo vehicle, with argon ion thrusters requiring operation in undesirable ranges of I_{sp} and efficiency. Propellant availability would indicate the use of krypton (ion) or hydrogen (MPD) for an effective lunar cargo vehicle. However, the use of argon ion thrusters in a non-optimal fashion for the lunar cargo vehicle must be considered, in order to fully exploit potential commonality between the lunar and Mars vehicles required for the full SEI mission plan. It has been shown in previous work¹ that even non optimal NEP lunar cargo vehicles using argon ion thrusters provide a mass benefit over the chemical aerobrake reference vehicle.

Payload Fraction Although the operational limits of thrusters sets lower limits on trip times, the power requirements tend to dominate the vehicle mass, and may result in relatively low payload fractions, as shown in Figures 3 and 4. For each thruster type, trip times less than 100 (10 kg/kWe) or 200 (20 kg/kWe) days result in precipitous declines in payload fraction.

Power Figures 5 and 6 show the marked effect of decreased trip time upon propulsion system power requirements. Although this penalty is severe on a single vehicle basis, it will be shown that for multiple uses of a lunar cargo vehicle, the power system mass penalty is ameliorated by the reduced propellant mass required for subsequent missions. For the purposes of comparison in a mission application context, a specific payload and lunar cargo mission scenario has been identified and compared to advanced chemical propulsion performance.

Lunar Cargo Mission Comparison

Mission Description

The results of the preceding analysis have been applied to the lunar cargo mission. A low-thrust ΔV of 8 km/s is assumed for the one way lunar transfer¹⁰. For comparison, the LEO - GEO orbit transfer ΔV , with a 28.5° inclination change, is 5.85 km/s³. The mission is assumed to be a delivery of cargo from Low Earth Orbit (LEO, 500 km) to a Low Lunar Orbit (LLO, 100 km), and the return to LEO of the empty vehicle. The optimization equations are applied to the outbound leg of the mission, where the payload fraction should be as high as possible. The return trip is not included in the optimization, because the additional propellant to return

the empty vehicle is only a small fraction of the total.

SEI mission studies of lunar cargo delivery have projected a delivery rate of one per year, so that only round trip times of a year or less are considered. In mission performance comparisons, a payload mass of 58 MT is assumed. The comparable chemical propulsion vehicle is based on results of the NASA 90-day Study for a cryogenic Hydrogen/Oxygen stage with aerobraking at Earth return¹¹. Optimized NEP lunar cargo vehicle mass performance and power requirements are shown in Figures 7 - 10. The NEP systems are compared to the chemical/aerobrake option on a basis of vehicle initial mass.

NEP Lunar Cargo Vehicle Performance

On a vehicle-to-vehicle basis, NEP lunar cargo vehicles are shown to be competitive with chemical aerobrake systems at relatively long trip times. 10 kg/kWe systems are competitive for trip times of greater than 100 (xenon, krypton ion) or 150 (argon ion, hydrogen MPD) days. Beyond 150 days, differences in thruster efficiencies have relatively small impact in vehicle mass. NEP lunar cargo vehicle mass is found to reach a minimal plateau of 70 - 80 tons at round trip times approaching a year, a mass savings of ~57% compared to the chemical/aerobrake reference vehicle.

The 20 kg/kWe NEP systems are competitive with the chemical systems at trip times greater than 200 days (ion propulsion) or 250 days (hydrogen MPD thrusters). At round trip times of 300 to 365 days, all thruster options result in vehicle initial masses of 90 - 100 MT, ~46% less than the chemical propulsion system. NEP mission performance is more sensitive to thruster efficiency at the higher specific masses, with the xenon and krypton thrusters showing better performance due to their higher efficiency at lower I_{sp} .

Minimum power requirements for the transportation of the 58 MT payload are calculated to range from 1 to 2 MWe for the 20 kg/kWe and 10 kg/kWe systems, respectively. The increase in power system mass tends to follow the increase in vehicle mass for short trip times. Maximum power levels for the round trip missions are 8 MWe at 50 to 100 days. Calculation of round trip power requirements or vehicle masses for very short trip times was limited by the sensitivity of the system parameters at short trip times. Beyond a minimum trip time, the iterative calculation of round trip power and propellant requirements ceased to converge.

The benefit of reusable NEP cargo vehicles is shown in Figure 11. The total mass required in LEO over 5 years of cargo delivery (1 mission/year) was calculated for both the NEP and the chemical/ aerobrake systems. In both cases, the vehicle is assumed reusable over the 5 year mission. In the case of the NEP vehicles, the annual resupply mass is the payload, propellant, and a new set of thrusters. In the case of the chemical/aerobrake system, resupply was taken to be payload and propellant. Even the aerobrake was assumed to be reusable.

The low propellant masses required by the high I_{sp} NEP systems results in a dramatic reduction in overall system mass requirements. The 10 kg/kWe systems in particular show significant reductions in mass over the chemical/aerobrake option, as high as 60%, for trip times as low as 100 days. The more conservative 20 kg/kWe system provides a similar benefit at longer trip times, on the order of 250 days or more.

Impacts of Mission Requirements Upon Technology

These optimized data, representing the best mission performance of NEP lunar cargo missions, indicate some areas of technology development which will enable the lunar cargo application:

Power/Propulsion Systems: Specific mass has a dramatic effect on mission performance, and also affects the optimum I_{sp} desired to achieve the mission. Low specific mass systems allow a wide range of thruster options to be considered, and provide the greatest mission benefit. Total power levels for the payloads considered in past lunar mission studies are 1 - 2 MWe for minimum mass systems. For faster transit times, power levels of 5 to 8 MWe may be required.

Thrusters: The optimal range of specific impulse needed to produce a lunar cargo vehicle which is competitive with conventional propulsion systems is from 3000 to 7000 seconds, depending on the desired trip time. Thruster input power levels of 100 - 1000 kWe may be needed to minimize system complexity by reducing the number of thrusters needed.

Reusability: The cumulative benefit of NEP for lunar cargo is greater than the benefit obtained on a mission by mission basis. The reuse of the NEP cargo vehicle should be considered to allow the most effective utilization of advanced propulsion.

Mars Missions

Mission Analysis

Mission analysis of interplanetary heliocentric trajectories does not allow simplifying assumptions of constant ΔV or continuous thrusting for system optimization. Instead, vehicle accelerations are comparable to the Sun's gravitational field, and the equations of motion must be computed and optimized numerically. Typically, this is done using variational calculus, with numerical solutions to the full three dimensional trajectory. Full trajectory optimization would also account for optimal launch dates. System optimization represents another level of optimization in addition to the trajectory optimization.

The mission performance of a low acceleration system such as NEP is determined by Equation 8¹².

$$1/M_f - 1/M_0 = (J a^2 dt) / 2P_e \eta \quad (8)$$

The term in parentheses is often referred to as the "J" parameter, and serves the same function as ΔV in impulse trajectories. In its purest sense, the J parameter is determined by the orbital mechanics of the mission, such as planetary alignment and desired trip time. This is true for the minimum J value, J_v , which optimizes the vehicle acceleration along the entire trajectory path. The minimal J solution assumes a vehicle operating at constant power, but with I_{sp} and thrust varied proportionately to obtain the optimal acceleration profile. In the past, numerous authors have solved this problem^{13,14}. However, I_{sp} values can vary over orders of magnitude in matching this minimum J trajectory program. Such variation is beyond the capability of many thruster concepts, and may introduce unwanted system complexity in those systems that can be designed to change I_{sp} .

The next best option to minimize propellant is to use a constant I_{sp} system, choosing I_{sp} such that the constant thrust J parameter, or J_c , is minimized. When performed properly, the optimal I_{sp} solution can yield J_c values within 12% of the minimum J_v ¹². This is a greater numerical challenge than the variable thrust solution, because coast times must be introduced to the analysis, and the optimum I_{sp} and power values must be found. Unlike the J_v analysis, the J_c optimization now requires iteration between the trajectory and the system to determine the optimal solution to the full parameter space of orbital mechanics and system performance. Typically, this involves a great deal of

iteration and trial-and-error analysis to reach the optimal solution.

Interplanetary low thrust mission analysis is thus plagued by the lack of an invariant parameter that characterizes the trajectory without involving system performance, as is the case with ΔV in impulsive mission design. Although the J_v parameter meets this need, it in effect assumes system characteristics which cannot be met by all types of electric propulsion. The J_c parameter is dependent on specific system characteristics.

As a potential solution, past researchers identified a new low thrust parameter, the characteristic length L, which was found to remain constant over a range of system characteristics¹⁵. This characteristic length value was found to be essentially independent of vehicle acceleration, and the value could be applied equally to constant or variable I_{sp} solutions. The use of this length parameter in one dimensional, field-free rectilinear motion analyses of low thrust systems allows simplified mission and systems analysis of a wide range of NEP system alternatives without resorting to the computational or conceptual complexity of full numerical calculus of variation solutions.

Characteristic Length

The use of the field-free, rectilinear approximations to low thrust propulsion depend on obtaining characteristic length values commensurate with the results of the calculus of variation solutions. Expressions for L are formulated using the rectilinear motion equations for either constant I_{sp} , thrust-coast-thrust trajectories, or for the variable I_{sp} case. In the case of the variable I_{sp} analysis, the relationship becomes simply¹²

$$L = (J_v t^3 / 12)^{1/2} \quad (9)$$

with J_v obtained from trajectory analysis. This method has the advantage that J_v is not dependent on system parameters, and only one trajectory must be calculated. The second option is to use the constant I_{sp} thrust-coast-thrust relationship

$$L = (c^2/a_0)(1 - \sqrt{(1 - a_0 t_p/c)})^2 - (t - t_p)(c/2) \ln(1 - a_0 t_p/c) \quad (10)$$

where

a_0 = initial acceleration

t_p = total propulsion time
 t = trip time
 with t_p obtained from trajectory analysis.

Optimal variable I_{sp} heliocentric trajectories were calculated for a range of trip times from 40 to 400 days using the Chebytop low thrust trajectory optimization program¹⁶. The 2015-2016 Earth to Mars opportunity was used, and the optimum launch date was determined for each trip time. The characteristic lengths were calculated using Equation 9. The results are shown in Figure 12. In addition, the characteristic length for constant I_{sp} trajectories of a 200 day, Earth to Mars heliocentric trajectory in the year 2016 is shown. The difference between the two values is 7%, an acceptable error when doing preliminary system optimization studies. Because of this close agreement, variable I_{sp} trajectory results were used to calculate characteristic length values. A cubic curve fit of characteristic length versus trip time was used in the optimization analysis:

$$L = 6.02 \times 10^{-13} * t^3 + 9.84 \times 10^{-6} * t^2 - 1240 * t + 6.13 \times 10^{10} \quad (11)$$

for characteristic length L in meters and trip time t in seconds.

System Optimization

The functional relationship between L and trip time was inserted into a systems optimization program to calculate optimum I_{sp} and power levels for Mars missions. The analyses described herein focussed only upon the heliocentric portion of the Earth-Mars trajectory. If a mission scenario requires optimization of the full trajectory, including planetary escape and capture spirals, a different set of optimal parameters will result. The differences between the two forms of optimization are discussed in a later section of this paper.

The rectilinear, field free equations of motion were used to calculate NEP system mission performance for the heliocentric trajectory. The principle mission performance parameter is the mass fraction, MF

$$MF = 1 - a_0 t_p / c \quad (12)$$

MF is dependent upon a_0 , t_p , and c ; however, t_p and c affect a_0 . a_0 is also affected by specific mass, trip time, and the characteristic length through the implicit equation

$$a_0 = 4c^2(1 - \sqrt{(1 - a_0 t_p / c) / (\ln(1 - a_0 t_p / c)(t - t_p) + 2c t_p + 2L)}) \quad (13)$$

Payload fraction is calculated from the mass fraction using the relation

$$\mu = MF - a_0 \alpha c / 2\eta \quad (14)$$

An additional parameter that may be calculated is the "effective ΔV ": $\Delta V = -c \ln(MF)$.

Input data required for the analysis are system specific mass, thruster efficiency - I_{sp} relationship, and desired trip time. Output is expressed in terms of payload fraction and power/payload ratio, as in the lunar cargo studies. Iteration is performed on the thrusting time and the specific impulse, with the optimum specific impulse determined by the maximum payload fraction point. The a_0 equation is solved using a bisection method. Presently, no tankage mass is accounted for in the analysis. This effect will be factored in to later system optimization analyses.

A comparison of results using the characteristic length method with the results of a full, calculus of variations optimization of trajectory, power, and specific impulse has been made for a system assuming 10 kg/kWe and argon ion thruster efficiency. The results of these two methods are compared in Figures 13 - 15. Figure 13 shows the optimum I_{sp} values calculated using the program QT2, which is based on the Chebytop program¹⁷, compared to the characteristic length calculations over a range of trip times from 150 to 400 days. Good agreement is seen for the lower trip times (150 - 250 days); at longer trip times, the two results diverge, with the characteristic length method estimating I_{sp} values up to 17% lower than the QT2 program. The reason for this divergence can be seen in the next two figures..

In both Figure 14 and 15, close agreement is found between the two methods, in spite of the difference in I_{sp} . This serves to indicate that for long trip times, greater than 250 days, the sensitivity of mission performance to I_{sp} is very low. The effects of a 17% difference in I_{sp} are negligible in terms of payload fraction and power ratio because the changes in vehicle mass due to propellant are small for such undemanding missions at high I_{sp} . It should also be noted that the QT2 calculations at long trip times resulted in all propulsive missions, whereas the characteristic length method calculated propulsive values of 70% - 80% of the total trip time. Characteristic length calculations at the all propulsive point resulted

in I_{sp} levels close to the QT2 values, with vanishingly small differences in payload fraction.

This comparison of results gives some confidence in the use of the characteristic length method for calculating optimal NEP system requirements and mission performance for Mars missions. The use of accurate trajectory analysis to develop the characteristic length values allows the trajectory optimization analysis to be removed from the system optimization calculations, allowing system designers to establish system performance requirements without iterating through repeated numerical calculation.

Optimization Results

Data obtained from this analysis allow assessment of specific systems and missions in terms of both optimal and off-optimal conditions. Some representative results of optimal analysis, calculated using argon ion thruster efficiencies, are shown in Figures 16, 18, and 20. Figure 16 shows the optimal specific impulse requirements over a range of trip times for both 5 and 10 kg/kWe systems. Figure 18 shows the resulting maximum payload fractions, while Figure 20 shows the power/payload ratios. The effect of specific mass is evident in the optimum I_{sp} and payload fraction values (Figures 16, 18). The lower payload fraction of the 10 kg/kWe systems results from the combination of increased power system mass and propellant mass, indicated by the comparable power ratio and lower I_{sp} values. The 10 kg/kWe system is found to be incapable of as low a trip time as the 5 kg/kWe system, which was able to complete a trip as fast as 100 days.

Similar results were obtained assuming a hydrogen MPD thruster. Mission performance for 5 and 10 kg/kWe systems is shown in Figures 17, 19, and 21. The lower projected efficiency of the MPD leads to somewhat decreased performance relative to the argon ion, yet both systems deliver high payload fractions for reasonable trip times. Some irregularities in the I_{sp} curve for the 5 kg/kWe case result from the discontinuity in the efficiency function model at an I_{sp} of ~ 7800 s. The increase in efficiency beyond 7800 seconds leads the optimization to desire higher I_{sp} than would be used with the lower I_{sp} efficiency function. In addition, MPD thruster I_{sp} was limited at the upper end to 10000 seconds, resulting in a plateau at the longest trip times.

For both systems, I_{sp} values of 4000 to 10000 seconds are desirable for maximizing payload fraction.

As in the lunar case, specific mass determines the optimal I_{sp} range for the mission. Power requirements tend toward the 10's of MWe per 100 MT payload, with sharp increases in power at the lowest trip times.

Orbital Escape and Capture Modelling

NEP planetary escape and capture can also be accounted for in a full mission analysis. A capability has been developed to optimize the low thrust mission to Mars including the spirals; due to space limitations this addition will only be mentioned briefly. Planetary escape and capture have been modelled as functions of vehicle acceleration by past researchers¹⁸ who developed the equations:

Planetary Escape:

$$\mu_e = \exp\{- (V_e/c)(1 - 0.805(a_0 R_{ce}^2/GM_p)^{1/4} \mu_e^{-1/4})\} \quad (15)$$

Planetary Capture:

$$\mu_c = \exp\{- (V_c/c)(1 - 0.805(a_0 R_{ce}^2/GM_p)^{1/4})\} \quad (16)$$

$\mu_{e,c}$ = payload fraction for escape, capture

G = Gravitational constant, $6.67 \times 10^{-11} \text{ m}^3/\text{s}^2\text{kg}$

R_{ce} = Circular Orbital radius for escape, capture; m

M_p = Planet mass; kg

$V_{e,c}$ = Circular Orbital Velocity for escape, capture; m/s

The full mission can be optimized iteratively by matching accelerations at escape and capture to those at the beginning and end of the heliocentric mission. The resulting optimal solution differs from comparable heliocentric only solutions. Payload fraction cannot be compared due to the additional propellant loads needed for escape and capture, but I_{sp} and normalized power are also affected, as shown in Figure(s) 22 and 23. The spiral escape and capture altitudes were 500 km at Earth and 20077 km at Mars, respectively. For the sake of comparison, these results are compared on the basis of heliocentric trip time. The inclusion of the planetary spirals in the analysis results in higher optimal I_{sp} and higher power-to-payload ratios than the heliocentric optimization.

Application to SEI Mars Missions

The status of Mars mission design for SEI missions is currently constantly changing. Two forms of SEI Mars mission are under consideration for NEP systems. The first is Mars cargo, typically a one-way delivery of large payload masses, with a reduced

emphasis on trip time. A high payload fraction is of primary concern in such a system. The optimal curves shown here are particularly suited to determining system and mission performance requirements for such a mission. The second mission application is round trip, piloted missions to Mars. The round trip nature of such a mission introduces additional variables into a mission/system optimization, such as stay time, total trip time, and payload jettison.

A myriad of piloted mission options exist^{1,2}, ranging from "split/sprint" missions with separate crew and cargo vehicles, to "all-up" missions with all payload on a single vehicle. In addition, two round trip mission modes may be considered: opposition and conjunction. Opposition missions are the most demanding, with short stay times at Mars requiring careful optimization of launch date. In the opposition mission, planetary alignments are unfavorable for one leg of the mission, increasing the propulsion system requirements and sensitivities. The second option, the conjunction mission, requires stay times of up to 2 years on Mars, but allows optimal transfer on both the outbound and inbound legs, minimizing propellant requirements. A minimum energy cargo mission would correspond to the outbound leg of a conjunction mission. Because of the variability in mission design for round trips, no analysis has been attempted using the characteristic length method.

Summary

Derivations of approximate systems/mission optimization techniques for lunar and Mars low thrust missions have been presented. These relationships are intended to provide systems analysts and mission designers with estimates of system requirements and mission performance without requiring access to detailed low thrust trajectory analysis codes.

Lunar optimization relations were achieved through the assumption of a constant ΔV spiral trajectory in Earth's gravity field, as well as an approximation to the exponential term in the payload fraction equation. Optimal I_{sp} values were calculated for two types of thruster, the ion and MPD. The efficiency - I_{sp} relationships of both types of thrusters were incorporated in the optimization. The equations were found to be accurate over a range of trip times; some departure from the exact solution was seen at trip times less than 60 - 100 days. This method may also be adopted for analyzing other orbital transfer missions which may be characterized by a constant ΔV . The optimal equations were then applied to a sample lunar

NEP mission and compared to past chemical aerobrake studies to determine the benefits of NEP to the lunar cargo mission.

Optimization of Mars systems were based on the characteristic length method for trajectory modelling. The characteristic length values for optimal Earth - Mars heliocentric trajectories in 2015 - 2016 were determined for a range of trip times. The nature of the characteristic length allows further analysis of NEP systems to be performed using algebraic equations derived from the field-free, rectilinear motion equations. Results of the approximate analysis were found to match closely with detailed heliocentric trajectory optimization results. Some divergence was found in optimal I_{sp} values at long trip times, due to the insensitivity of vehicle performance to variations in I_{sp} for long missions. Applications to SEI mission analysis were discussed.

Conclusions

In order to determine the most appropriate role for NEP technology in SEI missions, an ability to assess mission performance and determine the optimal operating regimes is required. It is hoped that the preceding relationships derived for orbital transfer and interplanetary travel will enable such analyses for future efforts in NEP system and mission analysis. NEP has been shown to have the potential to greatly benefit the Space Exploration Initiative, but further analyses and technology research are required to demonstrate these benefits.

Acknowledgements

The author wishes to express thanks to John Riehl and Kurt Hack of the Advanced Space Analysis Office of NASA Lewis Research Center for many fruitful discussions of heliocentric trajectory optimization, and Steven Oleson of Sverdrup Technology for discussions on orbital transfer optimization.

References

1. Hack, K.J., et al., "Evolutionary Use of Nuclear Electric Propulsion," AIAA Paper No. 90-3821, September, 1990.
2. Hack, K.J., George, J.A., and Dudzinski, L.A., "Nuclear Electric Propulsion Mission Performance for Fast Piloted Mars Missions," AIAA Paper No. 91-3488, September, 1991.

3. Jones, R. M., "Comparison of Potential Electric Propulsion Systems for Orbit Transfer," I. Spacecraft and Rockets, Vol. 21, No. 1, Jan.-Feb. 1984, pp. 88 - 95.
4. Auweter-Kurtz, M., Kurtz, H.L., and Schrade, H.O., "Optimization of Propulsion Systems for Orbital Transfer with Separate Power Supplies Considering Variable Thruster Efficiencies," AIAA Paper No. 85-1152, October, 1985.
5. Gilland, J.H., Myers, R.M., and Patterson, M.J., "Multimegawatt Electric Propulsion System Design Considerations," AIAA Paper No. 90-2552, July, 1990.
6. Riehl, J. H., et al., "Power and Propulsion Parameters for Nuclear Electric Vehicles," NASA Lewis Research Center Internal Document, July, 1988.
7. Wilbur, P., Beattie, J.R., and Hyman, J., "An Approach to the Parametric Design of Ion Thrusters," IEPC Paper No. 88-080, October, 1988.
8. Choueiri, E.Y., Kelly, A.J., and Jahn, R.G., "MPD Thruster Plasma Instability Studies," AIAA Paper No. 87-1067, May 1987.
9. George, J.A., "Multimegawatt Nuclear Power Systems for Nuclear Electric Propulsion," AIAA Paper No. 91-3607, September, 1991.
10. Palaszewski, B.P., "Lunar Transfer Vehicle Design Issues with Electric Propulsion Systems," AIAA Paper No. 89-2375, July, 1989.
11. Priest, C., and Woodcock, G., "Space Transportation Systems Supporting a Lunar Base," AIAA Paper No. 90-0422, 1990.
12. Melbourne, W. G., "Interplanetary Trajectories and Payload Capabilities of Advanced Propulsion Vehicles," JPL Technical Report No. 32-68, March, 1961.
13. Keaton, P., "Low-Thrust Rocket Trajectories," Los Alamos National Laboratory Report LA-10625-MS, March, 1987.
14. Melbourne, W., Sauer, C., "Payload Optimization for Power-Limited Vehicles," in Electric Propulsion Development, Vol. 9., Progress in Aeronautics and Astronautics, pp. 617 - 645., 1963.
15. Zola, C., "A Method of Approximating Propellant Requirements of Low-Thrust Trajectories," NASA TN D-3400, April, 1966.
16. Hahn, D.W. and Johnson, F.T., CHEBYTOP II - Chebychev Trajectory Optimization Program, NASA/OART Advanced Concepts and Missions Division Contract NAS2-5994, Final Report D180-12916-1, June 1971.
17. Riehl, J.P., and Mascy, A.C., "QT2 - A New Driver for the Chebytop System," Proposed Technical Memorandum, NASA Lewis Research Center, Cleveland, OH.
18. Ragsac, R., "Study of Trajectories and Upper Stage Propulsion Requirements for Exploration of the Solar System," Vol. II, Technical Report, Contract No. NAS2-2928, Final Report, September, 1967.

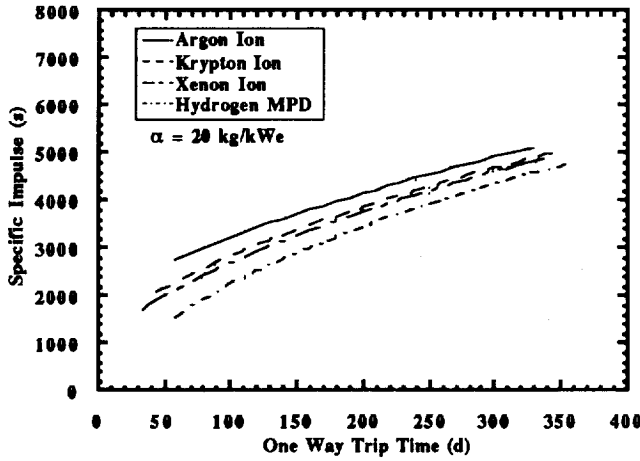


Figure 1. Optimized I_{sp} for NEP Lunar Cargo Vehicle, 20 kg/kWe system, no tankage.

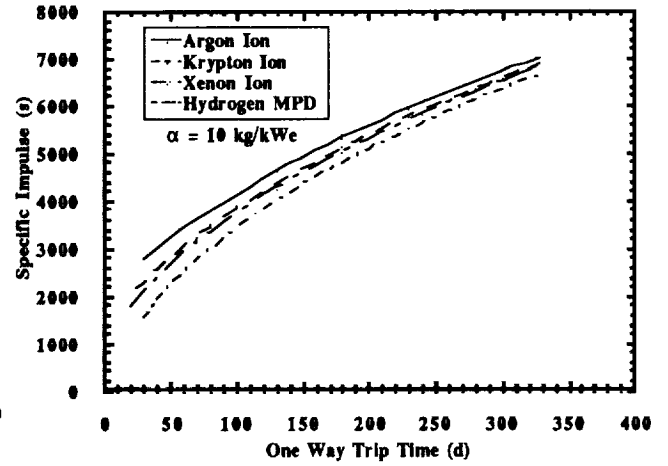


Figure 2. Optimized I_{sp} for NEP Lunar Cargo Vehicle, 10 kg/kWe, no tankage.

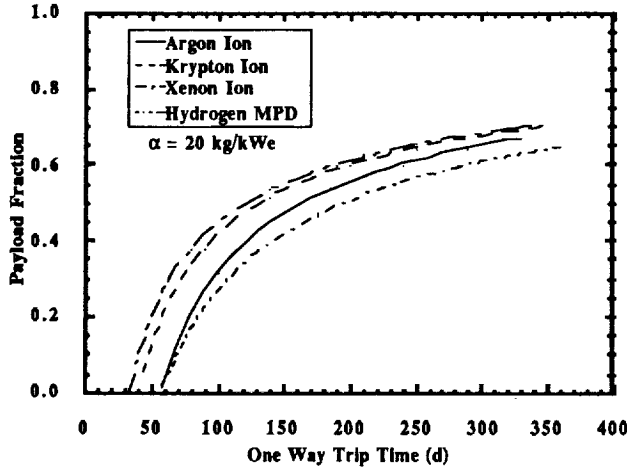


Figure 3. Optimized Payload Fraction for NEP Lunar Cargo Vehicle, 20 kg/kWe, no tankage.

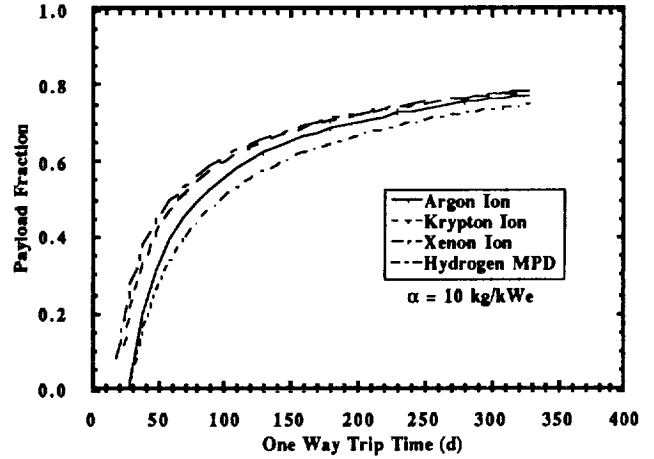


Figure 4. Optimized Payload Fraction for NEP Lunar Cargo Vehicle, 10 kg/kWe, no tankage.

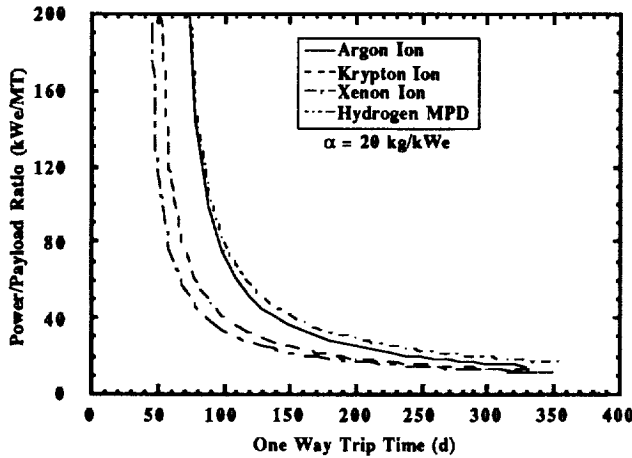


Figure 5. Optimized Power/Payload Ratio for NEP Lunar Cargo Vehicle, 20 kg/kWe, no tankage.

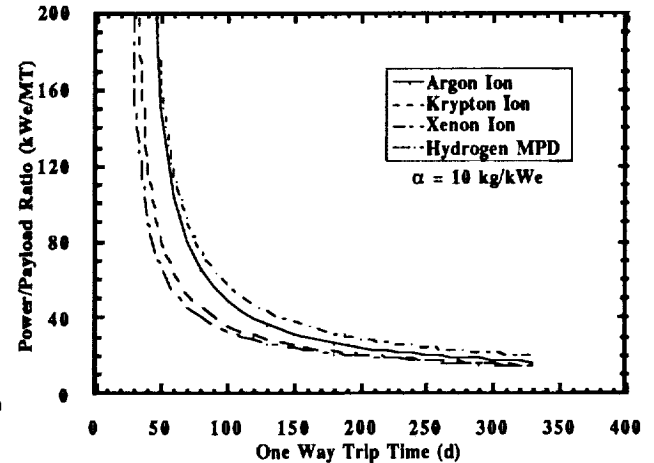


Figure 6. Optimized Power/Payload Ratio for NEP Lunar Cargo Vehicle, 10 kg/kWe, no tankage.

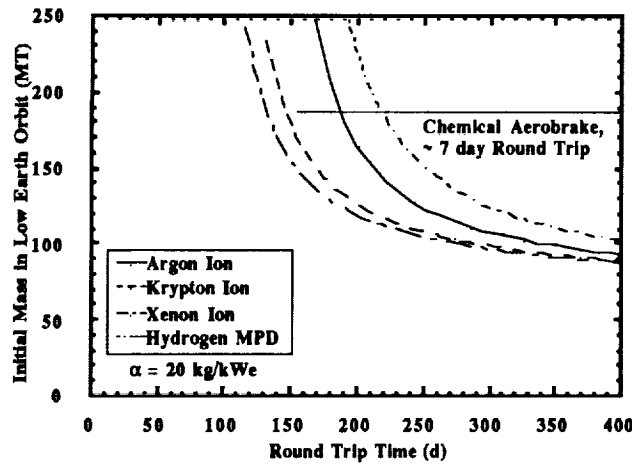


Figure 7. Optimized Lunar Cargo Vehicle Initial Mass in Low Earth Orbit, 20 kg/kWe NEP and Chemical/aerobrake systems (no tankage).

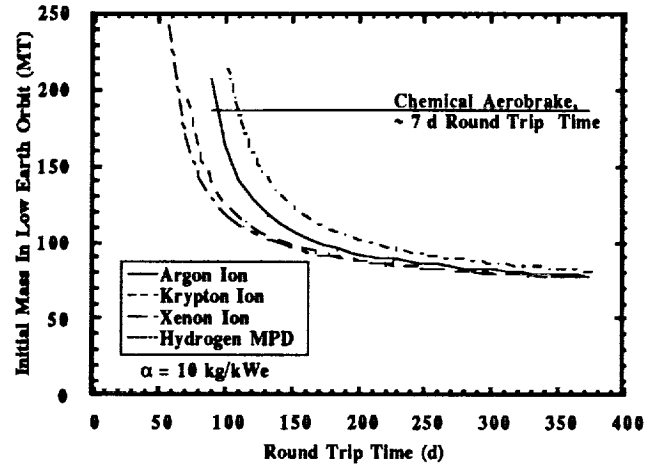


Figure 8. Optimized Lunar Cargo Vehicle Initial Mass in Low Earth Orbit, 10 kg/kWe NEP and Chemical/aerobrake systems (no tankage).

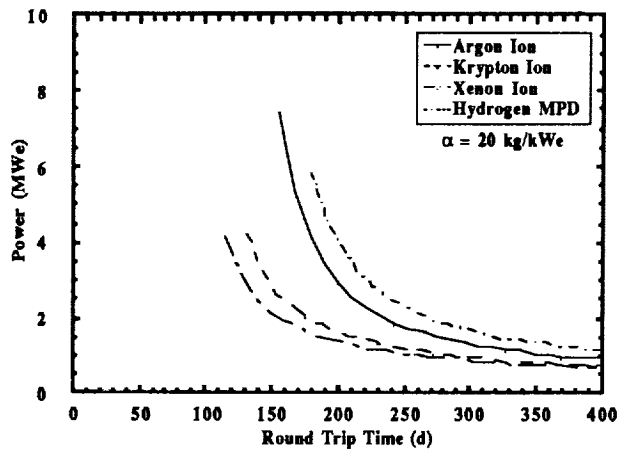


Figure 9. Optimized Power for Lunar Cargo Mission, 20 kg/kWe NEP system (no tankage).

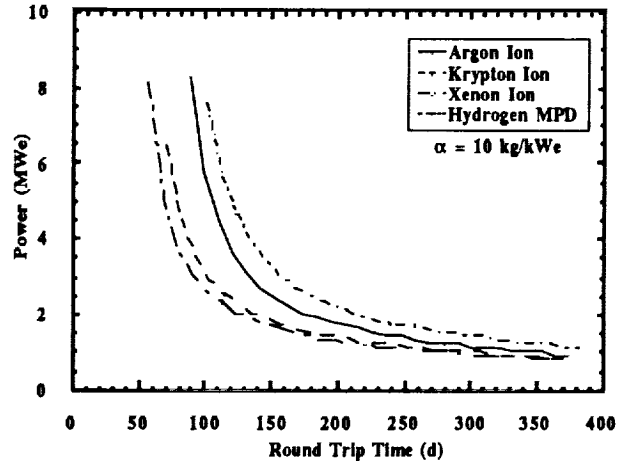


Figure 10. Optimized Power for Lunar Cargo Mission, 20 kg/kWe NEP system (no tankage).

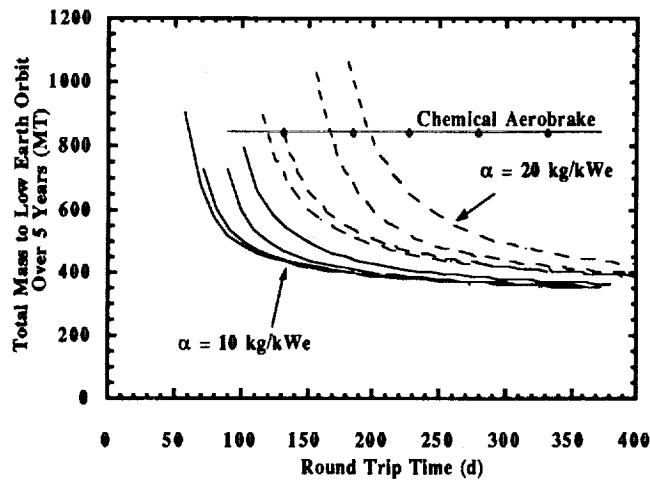


Figure 11. Overall NEP system performance for the Lunar Cargo Mission (no tankage).

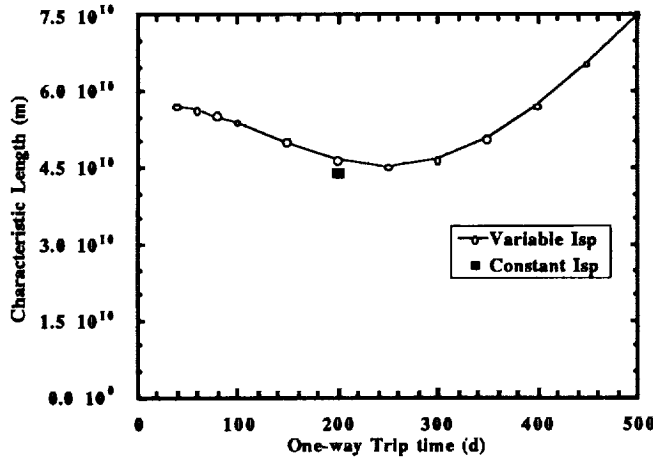


Figure 12. Characteristic Length Calculations for Variable and Constant I_{sp} Missions.

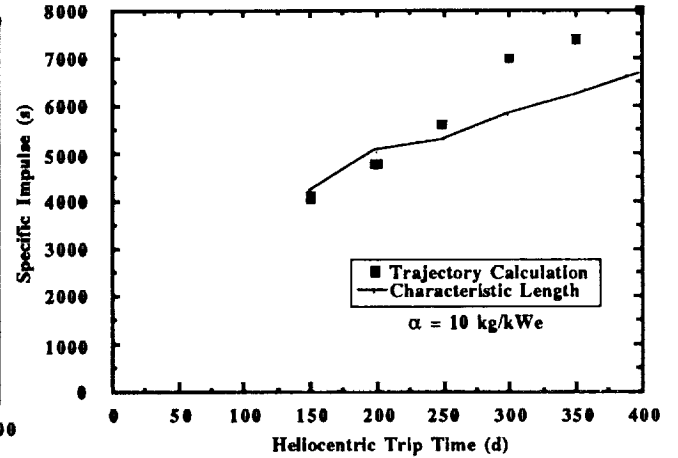


Figure 13. Comparison of optimum I_{sp} values obtained from characteristic length and exact methods.

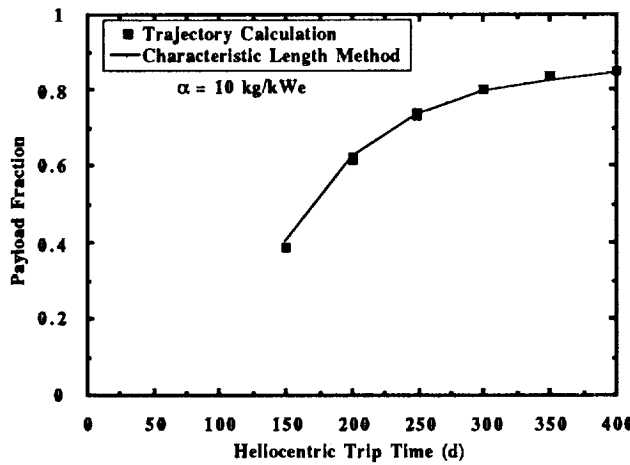


Figure 14. Comparison of optimum payload fraction values obtained from characteristic length and exact methods for the Mars mission.

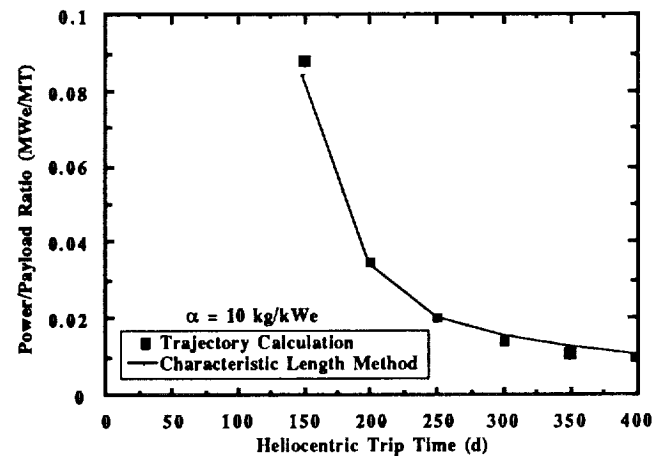


Figure 15. Comparison of optimum power requirements obtained from characteristic length and exact methods for the Mars mission.

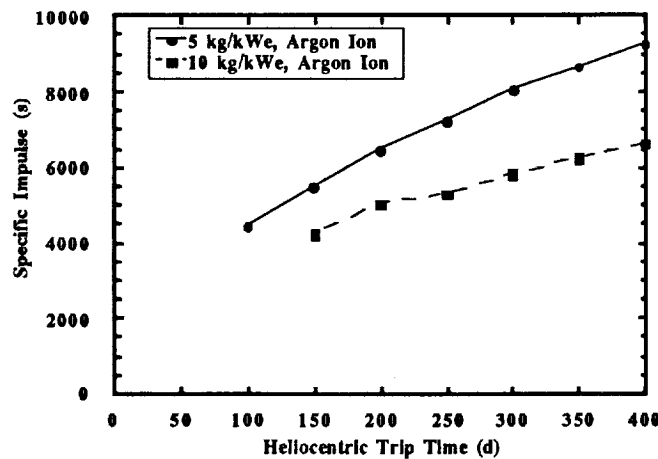


Figure 16. Optimal I_{sp} values for the Mars mission using argon ion thrusters.

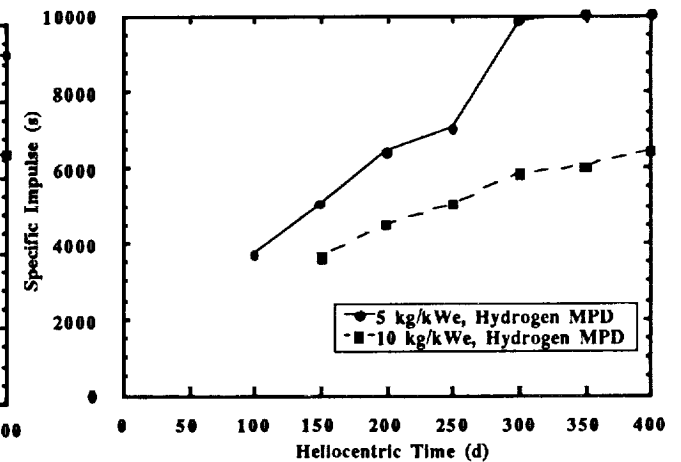


Figure 17. Optimal I_{sp} values for the Mars mission using hydrogen MPD thrusters.

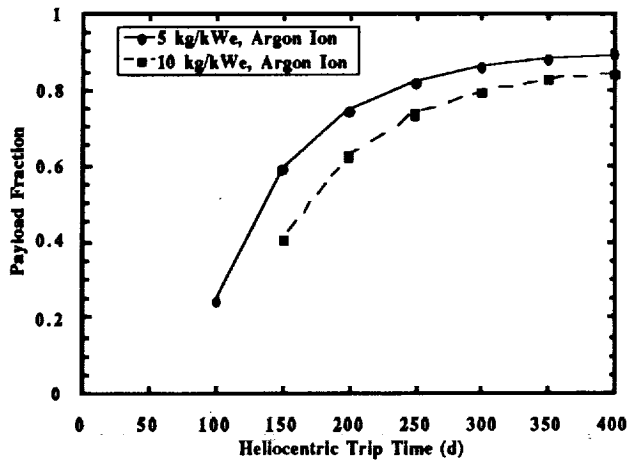


Figure 18. Optimum Payload Fraction values for the Mars mission using argon ion thrusters.

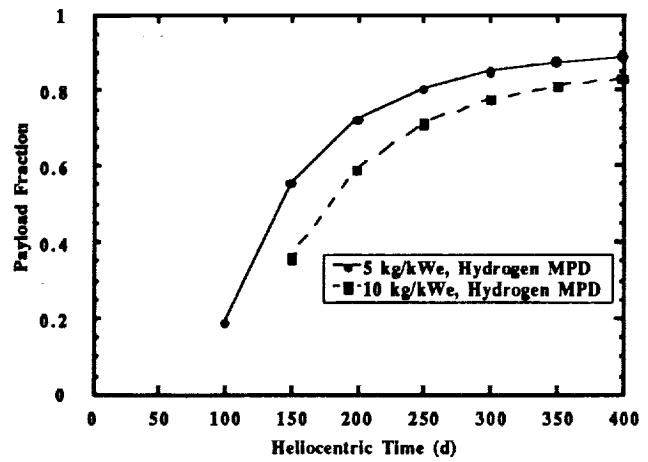


Figure 19. Optimum Payload Fraction values for the Mars mission using hydrogen MPD thrusters.

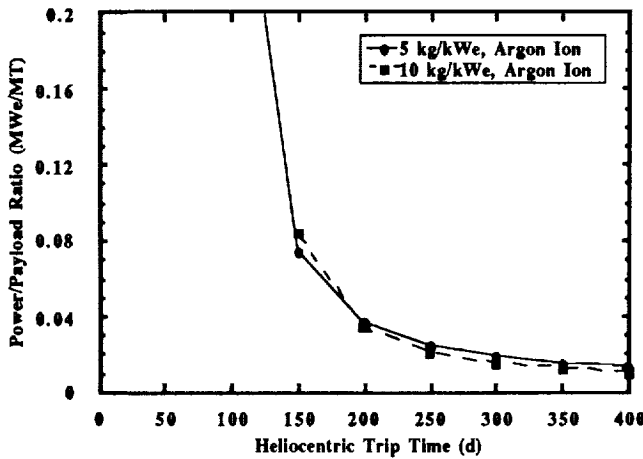


Figure 20. Optimal Power Requirements for the Mars mission using argon ion thrusters.

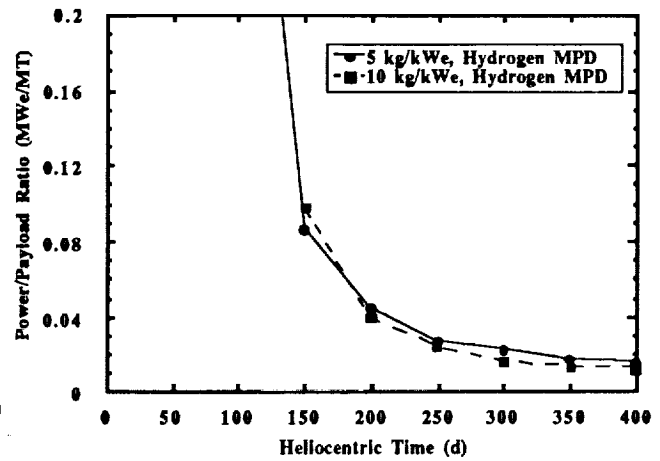


Figure 21. Optimal Power Requirements for the Mars mission using hydrogen MPD thrusters.

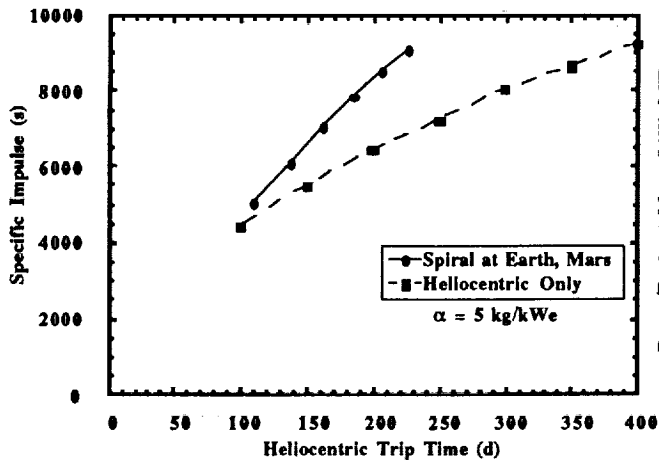


Figure 22. Effect of including spiral escape, capture upon I_{sp} optimization.

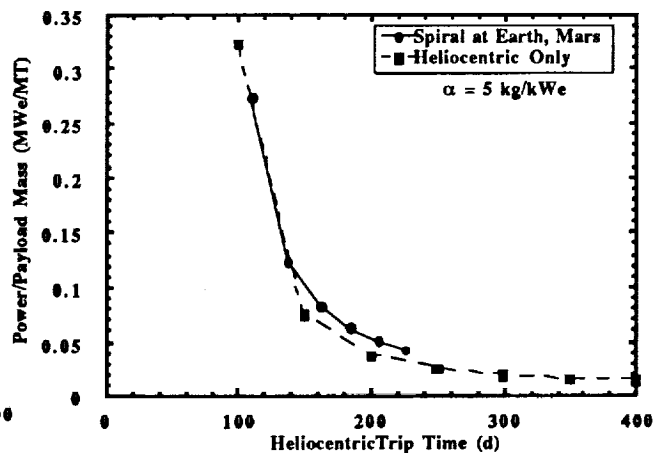


Figure 23. Effect of including spiral escape, capture upon Power Requirements.

REPORT DOCUMENTATION PAGE			Form Approved OMB No. 0704-0188	
Public reporting burden for this collection of information is estimated to average 1 hour per response, including the time for reviewing instructions, searching existing data sources, gathering and maintaining the data needed, and completing and reviewing the collection of information. Send comments regarding this burden estimate or any other aspect of this collection of information, including suggestions for reducing this burden, to Washington Headquarters Services, Directorate for Information Operations and Reports, 1215 Jefferson Davis Highway, Suite 1204, Arlington, VA 22202-4302, and to the Office of Management and Budget, Paperwork Reduction Project (0704-0188), Washington, DC 20503.				
1. AGENCY USE ONLY (Leave blank)	2. REPORT DATE December 1991	3. REPORT TYPE AND DATES COVERED Final Contractor Report		
4. TITLE AND SUBTITLE Mission and System Optimization of Nuclear Electric Propulsion Vehicles for Lunar and Mars Missions		5. FUNDING NUMBERS WU-None C-NAS3-25266		
6. AUTHOR(S) James H. Gilland				
7. PERFORMING ORGANIZATION NAME(S) AND ADDRESS(ES) Sverdrup Technology, Inc. Lewis Research Center Group 2001 Aerospace Parkway Brook Park, Ohio 44142		8. PERFORMING ORGANIZATION REPORT NUMBER E-6659		
9. SPONSORING/MONITORING AGENCY NAMES(S) AND ADDRESS(ES) National Aeronautics and Space Administration Lewis Research Center Cleveland, Ohio 44135-3191		10. SPONSORING/MONITORING AGENCY REPORT NUMBER NASA CR-189058 IEPC-91-038		
11. SUPPLEMENTARY NOTES Project Manager, John Clark, Nuclear Propulsion Office, NASA Lewis Research Center, (216) 977-7090. Prepared for the 22nd International Electric Propulsion Conference sponsored by AIDAA, AIAA, DGLR, and JSASS, Viareggio, Italy, October 14-17, 1991.				
12a. DISTRIBUTION/AVAILABILITY STATEMENT Unclassified - Unlimited Subject Category 20		12b. DISTRIBUTION CODE		
13. ABSTRACT (Maximum 200 words) The detailed mission and system optimization of low thrust electric propulsion missions is a complex, iterative process involving interaction between orbital mechanics and system performance. Through the use of appropriate approximations, initial system optimization and analysis can be performed for a range of missions. The intent of these calculations is to provide system and mission designers with simple methods to assess system design without requiring access or detailed knowledge of numerical, calculus of variations optimization codes and methods. Approximations for the mission/system optimization of Earth orbital transfer and Mars missions have been derived. Analyses include the variation of thruster efficiency with specific impulse. Optimum specific impulse, payload fraction, and power/payload ratios are calculated. The accuracy of these methods is tested and found to be reasonable for initial scoping studies. Results of optimization for Space Exploration Initiative lunar cargo and Mars missions are presented for a range of power system and thruster options.				
14. SUBJECT TERMS Electric propulsion; Mission analysis; Trajectory analysis; Nuclear electric propulsion		15. NUMBER OF PAGES 16		
		16. PRICE CODE A03		
17. SECURITY CLASSIFICATION OF REPORT Unclassified	18. SECURITY CLASSIFICATION OF THIS PAGE Unclassified	19. SECURITY CLASSIFICATION OF ABSTRACT Unclassified	20. LIMITATION OF ABSTRACT	